공학석사 학위논문

Thermal Hysteresis of Verwey Transition in Stoichiometric Magnetite Nanoparticles

마그네타이트 나노입자에서의 버웨이 트랜지션의 열적 히스테리시스

2016년 8월

서울대학교 대학원

화학생물공학부

홍 재 영

Abstract

Thermal Hysteresis of Verwey Transition in Stoichiometric Magnetite Nanoparticles

Jaeyoung Hong
School of Chemical and Biological Engineering
The Graduate School
Seoul National University

Metal-insulator transition in magnetite (Fe_3O_4), also called as Verwey transition, has been extensively studied. Recently, there has been increasing interest in the Verwey transition in Fe_3O_4 nanoparticles instead of bulk Fe_3O_4 with the hope of unraveling the mystery of this phenomenon. In this thesis, we report thermal hysteresis of Verwey transition in Fe_3O_4 nanoparticles for the first time, which has never been observed in bulk phase Fe_3O_4. Verwey transition observed in field-cooled (FC) measurements takes place at about 10 K lower than the transition

observed in zero-field-cooled (ZFC) measurements when the Fe_3O_4 nanoparticles are smaller than 120 nm. The difference between the two transition temperatures increases with increasing particle sizes below 42 nm. However, the transition temperatures do not change significantly within the size regime of 42 to 120 nm. The gap starts to diminish with particle size over 200 nm and disappears completely in the bulk phase. These findings may contribute to elucidating the mechanism of metal-insulator transition in Fe_3O_4.

Keywords : Verwey transition, magnetite nanoparticles, thermal hysteresis, size effect

Student number : 2014-22623

Contents

List of Figures

List of Tables

1. Introduction

1.1 Magnetite nanoparticles

For decades, nanomaterials have received significant attention for interesting features that are not observed in the bulk counterparts.[1-6] Synthesis of uniformly sized particles is very important since nanomaterial characteristics depend largely on their size.[1,7-9] So far, many successful syntheses of monodisperse nanoparticles have been reported using various methods including hot-injection,[7] thermal decomposition,[10] nonhydrolytic sol-gel[11] and polyol processes.[12,13] While a variety of nanoparticles with different materials have been reported, magnetite, which has a chemical formula of Fe_3O_4, has been widely used for its ferrimagnetic property with a Curie temperature of 858 K.[14-18] At room temperature, magnetite has an inverse spinel AB_2O_4 structure, composed of 24 iron atoms and 32 oxygen atoms in one unit cell. Eight Fe^{2+} ions occupy half of the octahedral B sites while sixteen Fe^{3+} ions occupy tetrahedral A sites and the remaining half of the octahedral B sites. Syntheses of monodisperse Fe_3O_4 nanoparticles with various shapes have been known for the last 20 years.[19-21] Iron oxide nanoparticles with different phase-dependent characteristics have been used in a wide range of applications such as magnetic resonance imaging (MRI) contrast agents, pathogen detection, and other biomedical applications.[22-28] In this report, we use the thermal decomposition of iron(III) acetylacetonate to prepare monodisperse magnetite nanoparticles which is easy to scale up.[19,29]

1.2 Verwey transition

Metal-insulator transition observed in highly stoichiometric Fe_3O_4, which is now called as Verwey transition, has intrigued many researchers due to their unknown mechanism since Verwey reported this transition in 1939.[30] Verwey transition occurs at around 120 K, which is then correspondingly called as the Verwey transition temperature (T_V). When the transition occurs, the crystal structure of magnetite changes from cubic ($Fd\bar{3}m$) above T_V to monoclinic (Cc) below T_V. This phase change is accompanied by a sharp increase in electrical resistance, a sharp decrease in magnetic moment, and anomalous heat capacity at T_V.[30-32] Verwey suggested the charge ordering of iron ions in B sites as the underlying mechanism of such a phenomenon. He argued that Fe^{2+} and Fe^{3+} ions in octahedral sites are delocalized at temperatures above T_V so that electrons can move by hopping. At temperatures below T_V, Fe^{2+} and Fe^{3+} ions are localized so that electrons cannot hop. However, skepticism arose and a long controversy over the charge ordering model did not die down until now.[33] Recently, Senn *et al.* claimed that a "trimeron" structure containing a linearly ordered arrangement of one Fe^{2+} ion and two Fe^{3+} ions plays a key role in the Verwey transition.[32,34]

Meanwhile, Verwey transition is extremely sensitive to the stoichiometry of magnetite. The transition is suppressed in cation-deficient magnetite and even it disappears altogether with slight deviation in the stoichiometry.[35,36] The failure in preparing a stoichiometric sample prevented scientists from elucidating the principles of Verwey transition. So far, most research regarding Verwey transition

were conducted with bulk phase magnetite.[31,32] Since the preparation of stoichiometric magnetite nanoparticles is challenging, investigations of Verwey transition in nanoparticles have only gained momentum in the last 15 years.[37-40] Recently, the effect of size on the Verwey transition in magnetite nanoparticles was reported.[29] The transition is suppressed when particles are smaller than a few tens of nanometers and disappears completely below 6 nm. In this thesis, we report the first observation of a thermal hysteresis in Verwey transition in stoichiometric magnetite nanoparticles.

2. Experimental Section

2.1 Materials

The following chemicals were purchased and used without further purification: benzyl ether (98%, Sigma Aldrich), oleic acid (technical grade, 90%, Sigma Aldrich), iron(III) acetylacetonate ($Fe(acac)_3$, 99+%, Acros Organics), iron(II,III) oxide (Puratronic, 99.997%, metals basis, Alfa Aesar). Ethyl alcohol (pure, 200 proof, anhydrous, ≥99.5%, Sigma Aldrich) and toluene (anhydrous, 99.8%, Sigma Aldrich) were bubbled with argon gas for 30 minutes before use.

2.2 Synthesis of stoichiometric magnetite nanoparticles

Stoichiometric magnetite nanoparticles were synthesized using a thermal decomposition method with a carbon monoxide (CO) gas mixture as a reducing agent with a typical Schlenk line technique.[19,20,29] Iron(III) acetylacetonate, oleic acid, and benzyl ether were mixed and degassed under vacuum for an hour. After degasification, the solution was heated to 290 ℃ at a rate of 20 ℃/min and then annealed at that temperature for 30 minutes with vigorous stirring while blowing a 4% CO/CO_2 (by mass) gas mixture. After the reaction, the solution was rapidly cooled to room temperature and washed with 200 ml of toluene and 500 ml of ethyl alcohol under an inert atmosphere. Washed particles were dried and stored in a glovebox. Nanoparticle size varied with the ratio of reactants used. 21.3 g of $Fe(acac)_3$ was added to 33.9 g of oleic acid and 312 g of benzyl ether to produce 42 nm

nanoparticles. If the amount of iron precursor was reduced to 13.85 g, 16 nm particles were produced. Nanoparticles larger than 100 nm were synthesized at a smaller scale. A mixture of 2.343 g of $Fe(acac)_3$, 3.39 g of oleic acid, and 31.2 g of benzyl ether resulted in 360 nm nanoparticles. 120 nm nanoparticles were produced with 1.917 g of iron precursor by bubbling pure CO gas through the solution to get monodisperse particles. Pure CO gas was also used in an attempt to get stoichiometric magnetite nanoparticles in the hundreds of nanometers region.

2.3 Stoichiometric bulk magnetite preparation

Iron(II,III) oxide purchased from Alfa Aesar was off-stoichiometric to show a suppressed Verwey transition. This bulk phase powder was annealed at 1300 ℃ for 24 hours while blowing pure CO gas to show a sharp Verwey transition at 124 K.

2.4 Characterization

Transmission electron microscopy (TEM) was conducted with a JEOL JEM-2010 electron microscope at an acceleration voltage of 200 kV. Powder X-ray diffraction (XRD) patterns were collected with a Rigaku D/MAX-3C diffractometer equipped with a Cu Kα (λ=1.54178 Å) radiation source. Magnetic properties were measured with a Quantum Design MPMS XL5 SQUID magnetometer under a magnetic field of 10 mT to observe the Verwey transition. The magnetic moment change in magnetite at around 100 - 120 K indicates a Verwey transition as a decrease in the magnetic moment coincides with structural change, electric conductivity decrease,

and anomalous heat capacity.[29] Both zero-field-cooled (ZFC) and field-cooled (FC) magnetization data were collected. First, the sample was cooled to 20 K without an applied field and then heated to 200 K with a magnetic field while acquiring magnetic data (ZFC measurements). After the heating measurement was completed, the sample was cooled again to 20 K with an external field while measuring magnetic properties simultaneously (FC measurements).

3. Results and Discussion

3.1 Synthesis of stoichiometric Fe_3O_4 nanoparticles

Stoichiometric magnetite nanoparticles were prepared with a previously reported synthesis scheme.[29] Modification of the magnetite nanocube synthesis scheme by exchanging argon for the carbon monoxide gas mixture resulted in successful synthesis of stoichiometric magnetite nanoparticles (Figures 1, 2).[20] Table 1 shows the average size, standard deviation, and Verwey transition temperature of synthesized nanoparticles. As-synthesized nanoparticles show a clear and sharp Verwey transition although the transition is suppressed slightly in the small size regime. In fact, magnetite nanoparticles showing Verwey transition can be obtained without a reducing atmosphere. Figures 3 and 4a show TEM images and magnetic moments of the magnetite nanoparticle synthesized without CO/CO_2 gas mixtures. Magnetite nanoparticles made with argon gas or ambient air show suppressed metal-insulator transition. The transition vanishes completely when the degassing procedure is omitted and ambient air is used instead of the CO/CO_2 gas mixture. As the Verwey transition is extremely sensitive to the ratio between iron and oxygen atoms in magnetite, a trace level of off-stoichiometry cannot be confirmed with a typical X-ray diffraction pattern (Figure 4b). The ratio of Fe^{2+} and Fe^{3+} ions, and therefore the ratio of iron and oxygen in Fe_3O_4, is dependent on the oxygen fugacity (f_{O_2}) during synthesis.[35] In a reducing environment, the f_{O_2} value is relatively low compared to the oxygen fugacity of an inert atmosphere. In that case, more Fe^{3+}

ions can be reduced to Fe^{2+} which otherwise would have remained as ferric ions. Since these nanoparticles show a sharp Verwey transition at around 120 K, it is plausible to assume that the CO/CO_2 mixture gas has enough reducing power to obtain a low oxygen fugacity value.[29]

On the other hand, 360 nm nanoparticles were off-stoichiometric and the Verwey transition was suppressed. The T_V measured in the ZFC condition was 119.4 K and the transition occurred at a broad range of temperatures. Using pure CO gas to induce a much lower oxygen fugacity during formation did not change the T_V of 119 K (Figure 5). Although synthesis using pure CO gas failed to make relatively large sized nanoparticles with sharp metal-insulator transition, we can infer from these results that the CO/CO_2 gas mixture was reductive enough to make stoichiometric nanoparticles in the tens of nanometers size range. The value of f_{O_2} has little effect when the oxygen fugacity is lower than a critical value.[35] From this, it can also be inferred that the CO/CO_2 gas mixture induces an f_{O_2} below the critical value.

3.2 Verwey transition dependent on measuring condition: ZFC and FC

Figure 6 shows the ZFC and FC magnetization data of various sizes of magnetite nanoparticles and the deoxidized bulk sample. In accord with a previous report, the T_V measured in ZFC decreased exponentially as the size became smaller. The 7 nm

nanoparticles did not show the Verwey transition because the blocking temperature was higher than the Verwey temperature in the few nanometers range. Nanoparticles larger than 42 nm show nearly sharp transition. Particles smaller than 42 nm show a slightly suppressed transition with a relatively low T_V.

However, there is a remarkable difference between Verwey transitions indicated in the ZFC and FC data. For bulk phase Fe_3O_4, two transitions in ZFC and FC data occur in the same way at the same temperature. The T_V in ZFC (T_{V_heat}) and FC data (T_{V_cool}) are nearly the same at 124.33 and 124.31 K, respectively. There is only a slight hysteresis in the M(H)-T curve (Figure 6h). Such hysteresis profiles have been known for a while but have received little attention since the hysteresis width was less than 1 K. The observed thermal hysteresis in the Verwey transition is considered to be negligible. On the contrary, in magnetite nanoparticles Verwey transition occurred at much lower temperature in FC versus ZFC measurements. T_{V_cool} was significantly lower than T_{V_heat}. For 42 nm nanoparticles, T_{V_cool} was 109.8 K while T_{V_heat} was 120.0 K. The 29 and 16 nm nanoparticles also showed a difference between T_{V_heat} and T_{V_cool} (ΔT_V), although the difference is less significant than that for larger sized nanoparticles. Even in 120 nm nanoparticles, whose characteristics are considered to be closer to bulk phase, T_{V_cool} was about 11 K lower than T_{V_heat}. Thermal hysteresis also existed in 360 nm nanoparticles, but ΔT_V was much smaller than that of correspondingly smaller sized particles. Meanwhile, there was no sign of Verwey transition for 7 nm nanoparticles in either the ZFC or FC data.

Stoichiometric bulk magnetite was oxidized to investigate whether off-stoichiometry was a cause for thermal hysteresis instead of the size (Figure 7). However, thermal hysteresis was not observed in the oxidized bulk magnetite where the Verwey transition was suppressed due to the off-stoichiometry. Sample quality was not the cause of thermal hysteresis in the Verwey transition.

Figure 8 shows the Verwey transition temperature measured in ZFC and FC conditions for various magnetite nanoparticles and the stoichiometric bulk sample. The change in T_{V_cool} differed from that of T_{V_heat}. T_{V_cool} did not increase exponentially with the size of the nanoparticles. The Verwey transition temperature measured in the cooling condition did not change significantly within size regime of 42 to 120 nm. Instead, the profile suggests that T_{V_cool} increases as the size becomes smaller than 42 nm. Although the 360 nm nanoparticles appear to be off-stoichiometric, we suppose the gap between the two transition temperatures starts to be reduced at a certain critical size below 300 nm given the overall tendency of ΔT_V. Figure 9 shows the ZFC and FC magnetization data of a mixture of 120 and 220 nm nanoparticles. Since T_{V_heat} values were nearly the same in all nanoparticles larger than 42 nm, ZFC data were acquired as expected. In contrast, Verwey transition shows a two-step-like behavior in FC magnetization data. One step located at 121.1 K and the other at 110.9 K. Considering the value of ΔT_V for relatively monodisperse 120 nm nanoparticles, which is about 11 K (Figure 6f), it is reasonable to hypothesize that the transitions at 110.9 K and 121.1 K come from the 120 and 220 nm nanoparticles, respectively. We conjecture that there might be a

critical size around 200 nm where T_{V_cool} starts to increase to finally get closer to T_{V_heat} as the size increases. Thermal hysteresis becomes insignificant as the size grows beyond the 'flat' region where the ΔT_V value does not vary regardless of the nanoparticles size. We presume that magnetic domain structure of nanoparticles may have some role in this discrepancy between the transitions under different measuring conditions. Cubic magnetite has a critical grain size of about 100 nm, which delineates a single-domain from a multi-domain structure.[41] More studies are needed to clarify these fundamental questions.

4. Conclusion

In conclusion, a remarkable thermal hysteresis of the Verwey transition in stoichiometric magnetite nanoparticles was observed and reported for the first time. Stoichiometric magnetite nanoparticles with sizes between 7 and 360 nm were synthesized and their Verwey transition was studied by collecting magnetization data. While Verwey transition temperatures of ZFC data followed the previous report, the T_V values from FC data were lower than that T_{V_heat} for all nanoparticle sizes. The change in T_{V_cool} values was quite different from that of T_{V_heat} values. The gap between T_{V_cool} and T_{V_heat} became larger when the size increased from 7 to 42 nm, and then remained unchanged before diminishing completely for nanoparticles exceeding a few hundreds of nanometers. Although the reason for why the thermal hysteresis of Verwey transition exists only in Fe_3O_4 nanoparticles is still unknown, this novel finding may aid in understanding the principles of the Verwey transition.

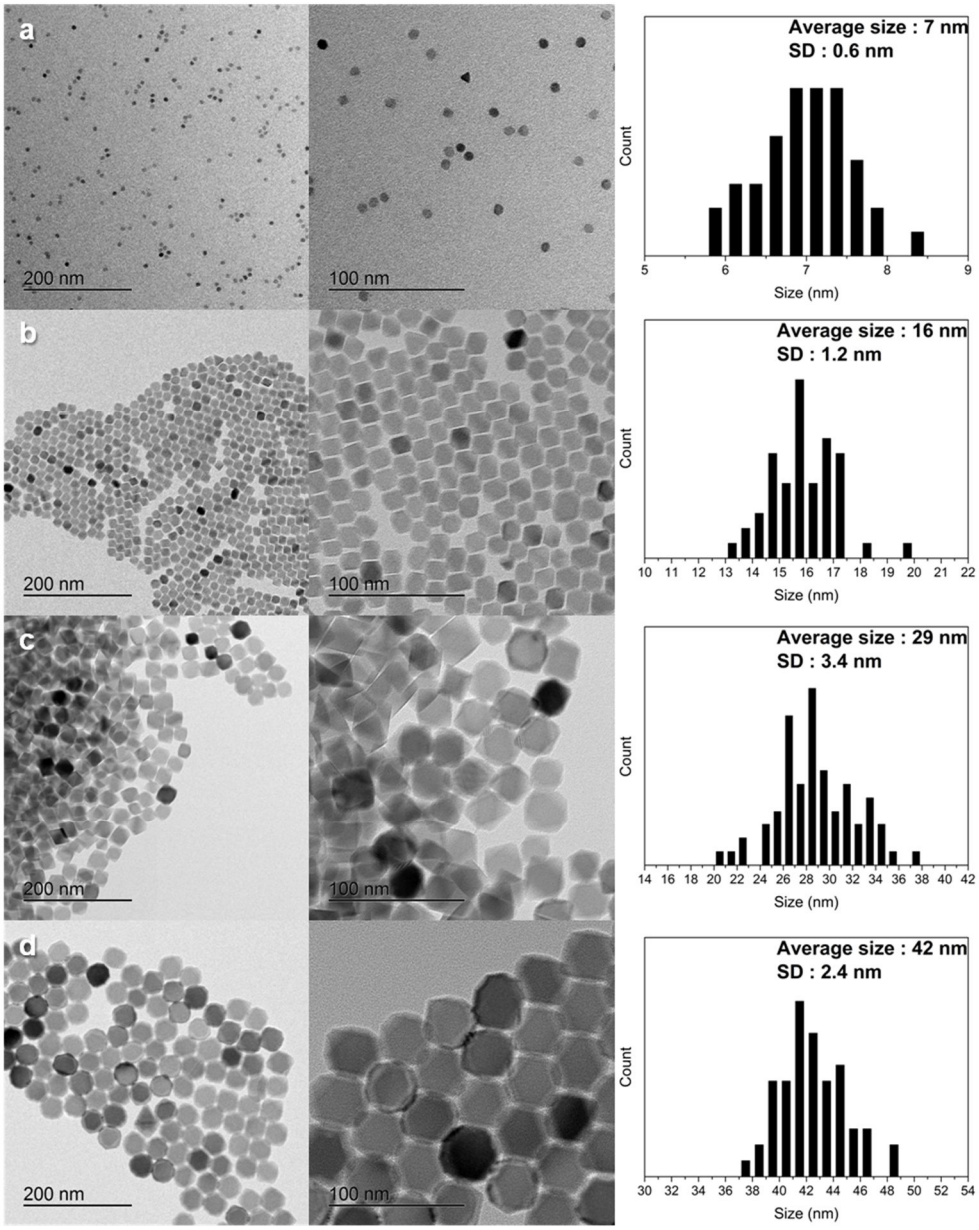

Figure 1. TEM images and size distribution histograms of (a) 7 (b) 16 (c) 29 (d) 42 nm Fe_3O_4 nanoparticles.

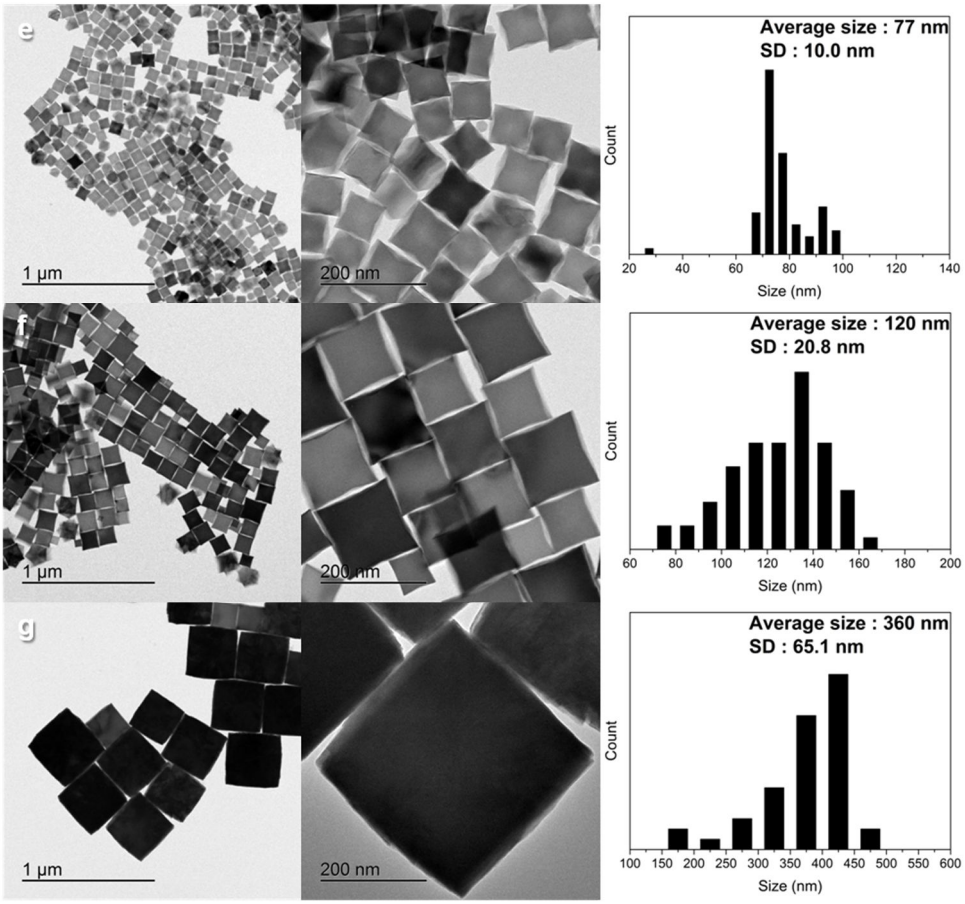

Figure 1. (continued) TEM images and size distribution histograms of (e) 77 (f) 120 and (g) 360 nm Fe_3O_4 nanoparticles.

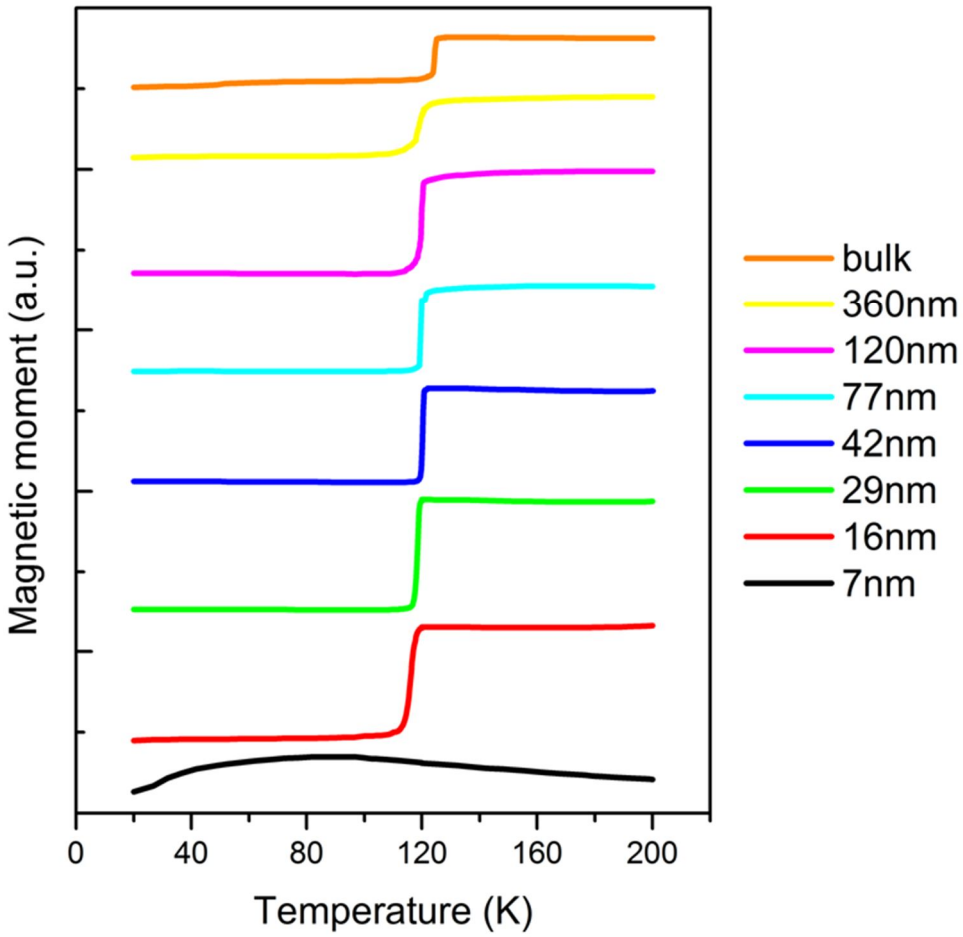

Figure 2. ZFC magnetization data of Fe_3O_4 nanoparticles and stoichiometric bulk Fe_3O_4.

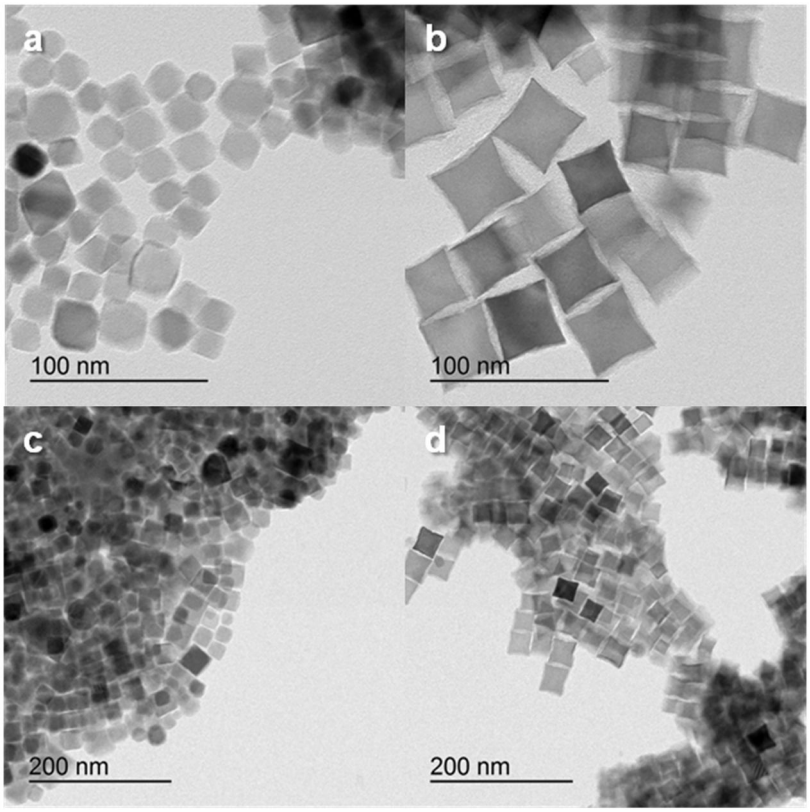

Figure 3. TEM images of Fe_3O_4 nanoparticles synthesized with (a) argon gas (b) ambient air (c) argon gas without a degassing process and (d) ambient air without a degassing process.

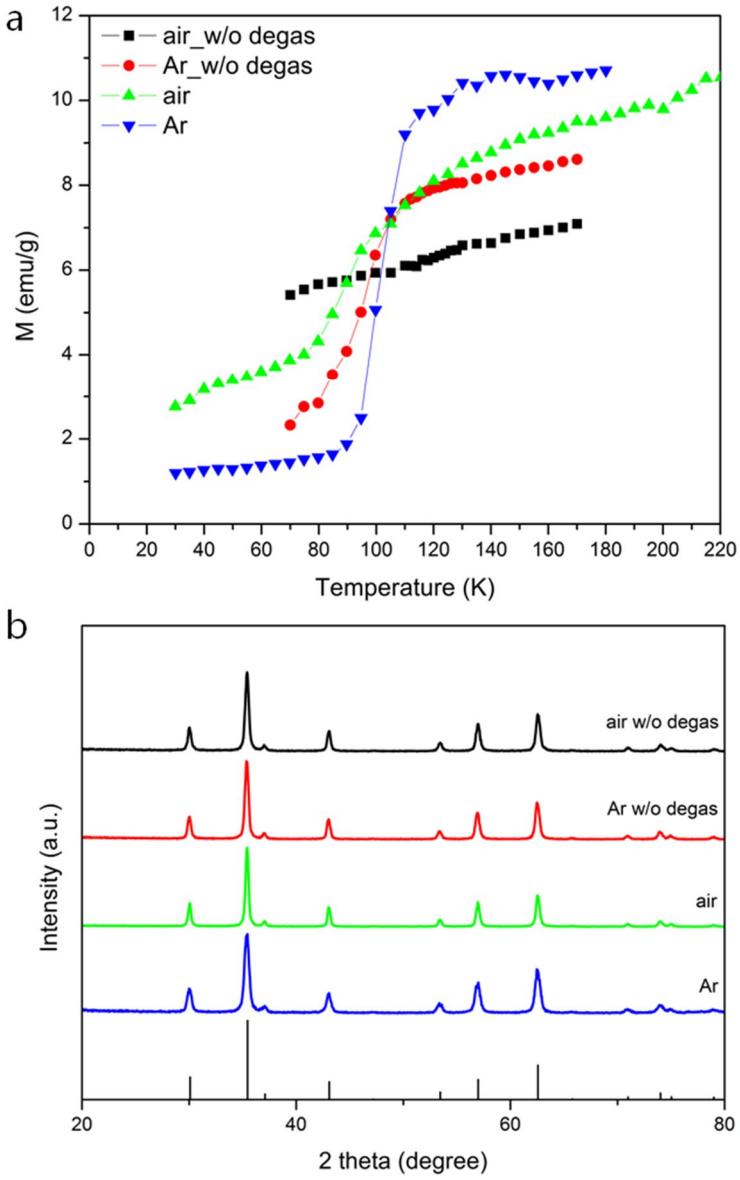

Figure 4. (a) Magnetic moment and (b) XRD patterns of off-stoichiometric Fe_3O_4 nanoparticles with a reference bulk Fe_3O_4 pattern. (JCPDS #19-629)

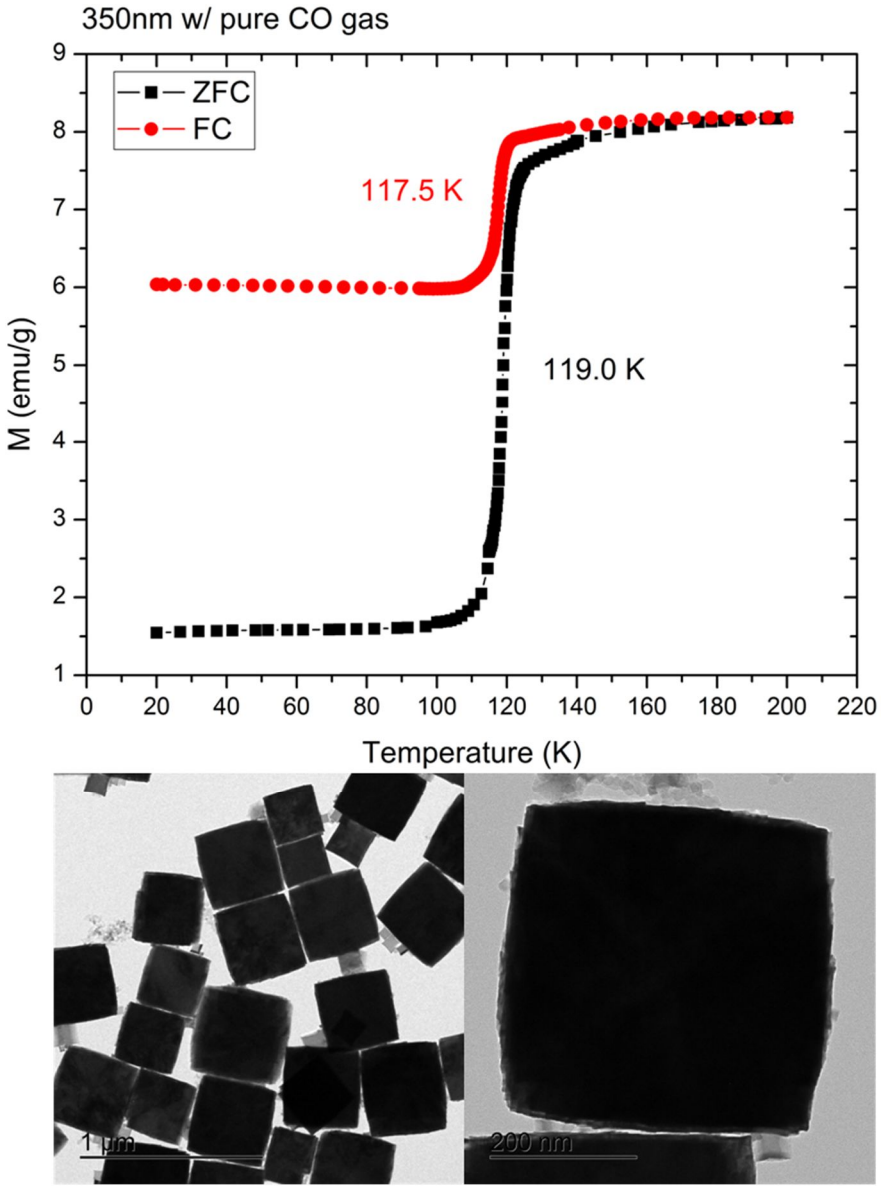

Figure 5. Magnetic moment and TEM images of 350 nm Fe_3O_4 nanoparticles synthesized with pure CO gas.

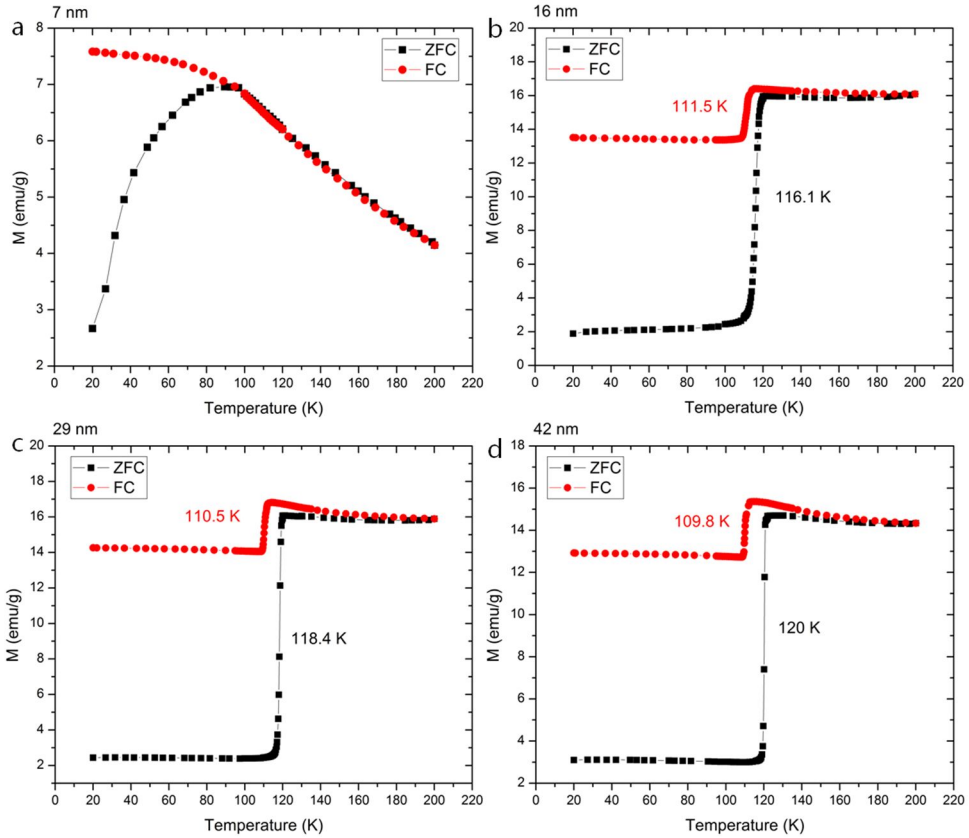

Figure 6. Zero-field-cooled (ZFC) and field-cooled (FC) magnetization data of (a) 7 (b) 16 (c) 29 (d) 42 nm Fe_3O_4 nanoparticles.

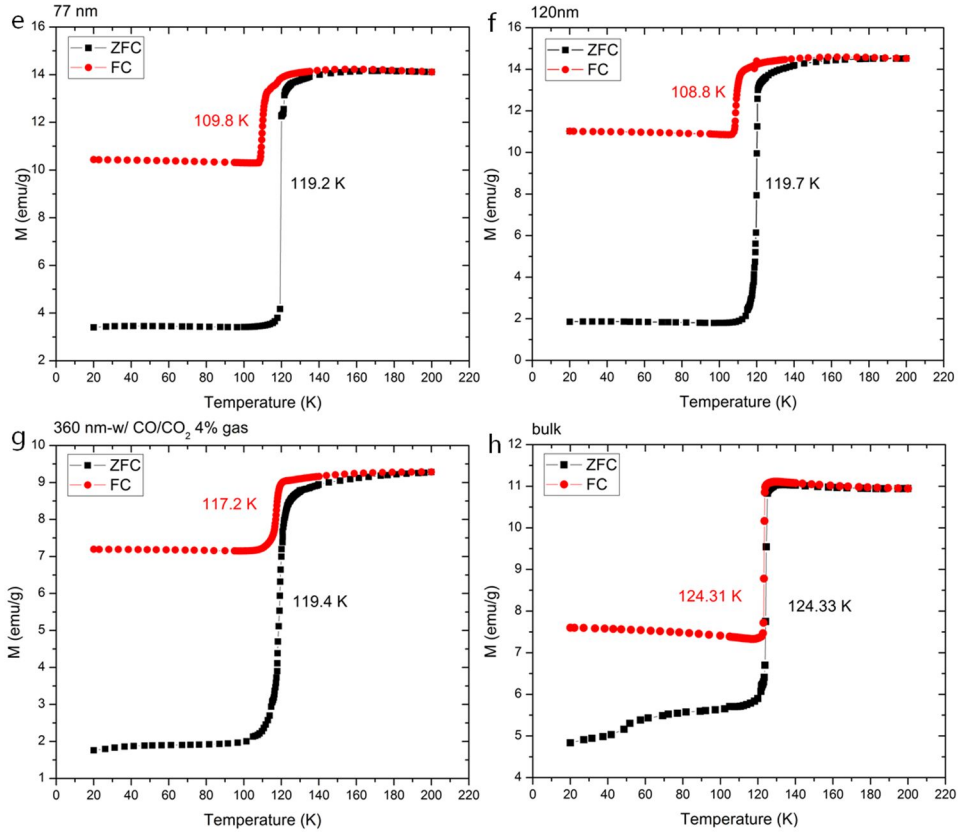

Figure 6. (continued) Zero-field-cooled (ZFC) and field-cooled (FC) magnetization data of (e) 77 (f) 120 (g) 360 nm Fe_3O_4 nanoparticles and (h) stoichiometric bulk Fe_3O_4.

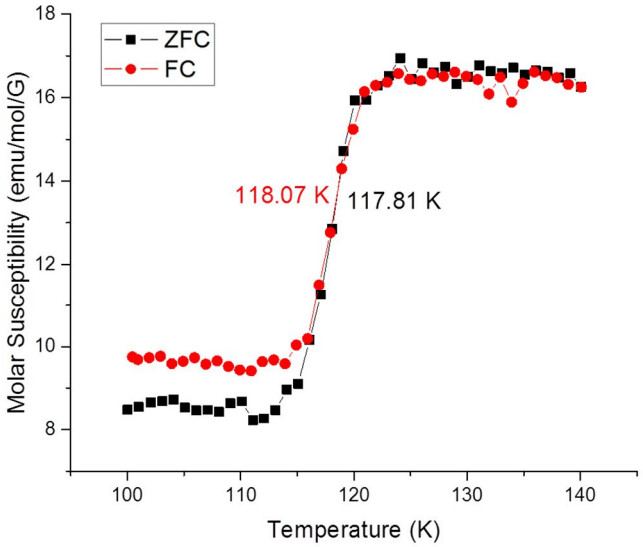

Figure 7. ZFC/FC curve of oxidized bulk magnetite. The bulk sample was oxidized at 473 K under ambient atmosphere for 6 days.

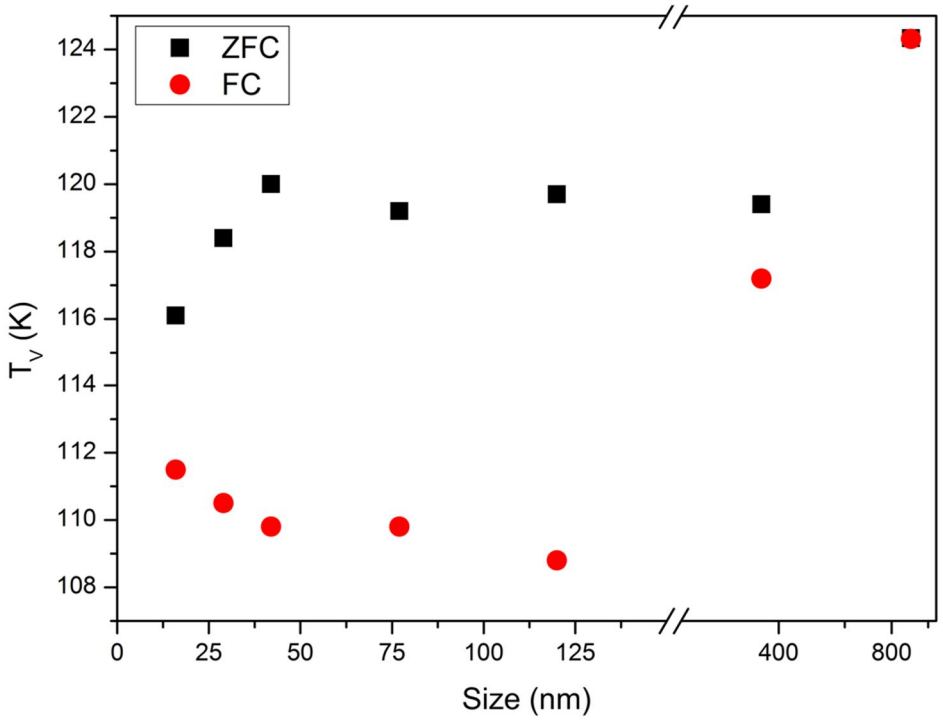

Figure 8. Verwey transition temperatures in ZFC and FC measurements of several magnetite nanoparticles and stoichiometric bulk sample.

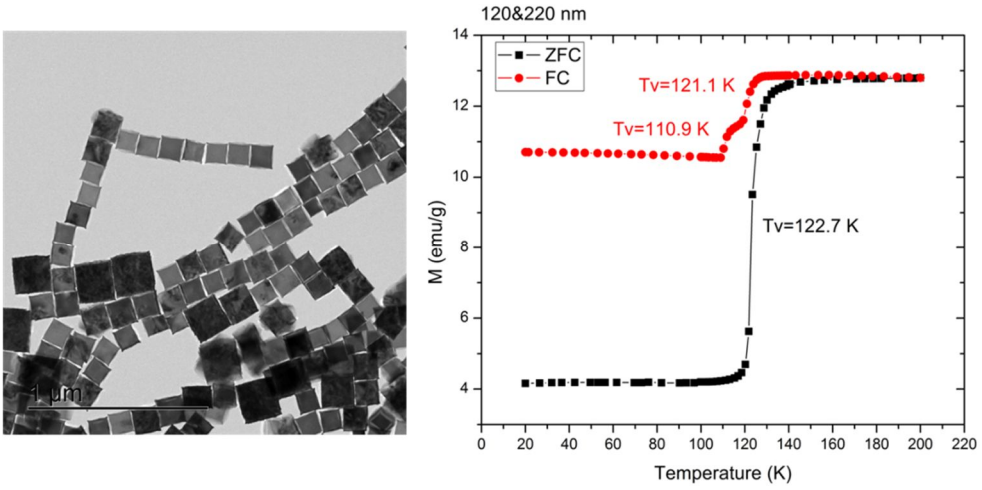

Figure 9. TEM image and ZFC and FC magnetic data of a mixture of 120 and 220 nm nanoparticles.

Table 1. Standard deviation and Verwey transition temperature from ZFC and FC magnetization data collected from various sized nanoparticles.

Size (nm)	Standard deviation (nm)	T_{V_heat} (K)	T_{V_cool} (K)
Bulk	-	124.33	124.31
364	65.1	119.4	117.2
120	20.8	119.7	108.8
77	10.0	119.2	109.8
42	2.4	120	109.8
29	3.4	118.4	110.5
16	1.2	116.1	111.5
7	0.6	-	-

References

[1] Alivisatos, A. P. *Science* **1996**, 271, 933.

[2] Majetich, S. A.; Jin, Y. *Science* **1999**, 284, 470.

[3] Lu, A. H.; Salabas, E.L.; Schüth, F. *Angew. Chem., Int. Ed.* **2007**, 46, 1222.

[4] Murray, C. B.; Kagan, C. R.; Bawendi, M. G. *Science* **1995**, 270, 1335.

[5] Goesmann, H.; Feldmann, C. *Angew. Chem., Int. Ed.* **2010**, 49, 1362.

[6] Zarur, A.; Ying, J. *Nature* **2000**, 403, 65.

[7] Murray, C. B.; Noms, D. J.; Bawendi, M. G. *J. Am. Chem. Soc*. **1993**, 115, 8706.

[8] Weller, H. *Angew. Chem., Int. Ed.* **1993**, 32, 41.

[9] Klabunde, K. J. *Nanoscale Materials in Chemistry*, John Wiley & Sons, Inc., New York, **2001**.

[10] Rockenberger, J.; Scher, E. C.; Alivisatos, A. P. *J. Am. Chem. Soc*. **1999**, 121, 11595.

[11] Vioux, A. *Chem. Mater.* **1997**, 9, 2292.

[12] Sun, Y.; Xia, Y. *Adv. Mater*. **2002**, 14, 833.

[13] Park, J.; Joo, J.; Kwon, S. G.; Jang, Y.; Hyeon, T. *Angew. Chem., Int. Ed.* **2007**, 46, 4630.

[14] Sun, S.; Murray, C. B.; Weller, D.; Folks, L.; Moser, A. *Science* **2000**, 287, 1989.

[15] Noh, S. H.; Na, W.; Jang, J. T.; Lee, J. H.; Lee, E. J.; Moon, S. H.; Lim, Y.; Shin, J. S.; Cheon, J. *Nano Lett.* **2012**, 12, 3716.

[16] Kim, Y.; Lee, C.; Shim, I.; Wang, D.; Cho, J. *Adv. Mater.* **2010**, 22, 5140.

[17] Zeng, H.; Black, C. T.; Sandstrom, R. L.; Rice, P. M.; Murray, C. B.; Sun, S. *Phys. Rev. B* **2006**, 73, 020402.

[18] Zhang, D.; Liu, Z.; Han, S.; Li, C.; Lei, B.; Stewart, M. P.; Tour, J. M.; Zhou, C. *Nano Lett.* **2004**, 4, 2151.

[19] Sun, C.; Zeng, H. *J. Am. Chem. Soc*. **2002**, 124, 8204.

[20] Kim, D.; Lee, N.; Park, M.; Kim, B. H.; An, K.; Hyeon, T. *J. Am. Chem. Soc*. **2009**, 131, 454.

[21] Park, J.; An, K.; Hwang, Y.; Park, J. G.; Noh, H. J.; Kim, J. Y.; Park, J. H.; Hwang, N. M.; Hyeon, T. *Nat. Mater.* **2004**, 3, 891.

[22] Gu, H.; Xu, K.; Xu, C.; Xu, B. *Chem. Commun.* **2006**, 941.

[23] Bulte, J. W.; Kraitchman, D. L. *NMR Biomed.* **2004**, 17, 484.

[24] Xie, J.; Chen, K.; Lee, H. -Y.; Xu, C.; Hsu, A. R.; Peng, S.; Chen, X.; Sun, S. *J. Am. Chem. Soc*. **2008**, 130, 7542.

[25] Laurent, S.; Forge, D.; Port, M.; Roch, A.; Robic, C.; Elst, L. V.; Muller, R. N. *Chem. Rev.* **2008**, 108, 2064.

[26] Xie, J.; Liu, G.; Eden, H. S.; AI, H.; Chen, X. *Acc. Chem. Res*. **2011**, 44, 883.

[27] Lee, N.; Choi, Y.; Lee, Y.; Park, M.; Moon, W. K.; Choi, S. H.; Hyeon, T. *Nano Lett.* **2012**, 12, 3127.

[28] Stanley, S. A.; Gagner, J. E.; Damanpour, S.; Yoshida, M.; Dordick, J. S.; Friedman, J. M. *Science* **2012**, 336, 604.

[29] Lee, J.; Kwon, S. G.; Park, J. -G.; Hyeon, T. *Nano Lett.* **2015**, 15, 4337.

[30] Verwey, E. J. *Nature* **1939**, 144, 327.

[31] Walz, F. *J. Phys.: Condens. Matter* **2002**, 14, R285.

[32] Senn, M. S.; Wright, J. P.; Attfield, J. P. *Nature* **2012**, 481, 173.

[33] García, J.; Subías, G. *J. Phys.: Condens. Matter* **2004**, 16, R145.

[34] Senn, M. S.; Wright, J. P.; Cumby, J.; Attfield, J. P. *Phys. Rev. B* **2015**, 92, 024104.

[35] Aragón, R.; Buttrey, D. J.; Shepherd, J. P.; Honig, J. M. *Phys. Rev. B* **1985**, 31, 430.

[36] Kąkol Z.; Honig, J. M. *Phys. Rev. B* **1989**, 40, 9090.

[37] Mitra, A.; Mohapatra, J.; Meena, S. S.; Tomy, C. V.; Aslam, M. *J. Phys. Chem. C* **2014**, 118, 19356.

[38] Yu, Q.; Mottaghizadeh, A.; Wang, H.; Ulysse, C.; Zimmers, A.; Rebuttini, V.; Pinna, N.; Aubin, H. *Phys. Rev. B* **2014**, 90, 075122.

[39] Wang, J.; Chen, Q.; Li, X.; Shi, L.; Peng, Z.; Zeng, C. *Chem. Phys. Lett.* **2004**, 390, 55.

[40] Guigue-Millot, N.; Keller, N.; Perriat, P. *Phys. Rev. B* **2001**, 64, 012402.

[41] Butler, R. F.; Banerjee, S. K. *J. Geophys. Res.* **1975**, 80, 4049.

초록

마그네타이트 (Fe_3O_4) 에서 나타나는 금속-절연체 전이 현상은 버웨이 트랜지션 (Verwey transition) 으로 불리며 오랜 시간 많은 과학자들에 의해 연구되었다. 최근에 화학량론적 마그네타이트 나노입자의 합성이 가능해지며, 벌크 물질에만 국한되어있던 버웨이 트랜지션 연구가 나노입자까지 확장되었다. 본 연구에서는 벌크 물질에서는 관측된 적이 없는 버웨이 트랜지션의 열적 히스테리시스를 나노입자에서 처음으로 발견하였다. 나노입자가 120 nm 보다 작을 때, 냉각 과정에서의 버웨이 트랜지션은 가열 과정에서의 전이보다 10 K 정도 낮은 온도에서 일어났다. 입자가 42 nm 보다 작을 때는 크기가 커지면서 두 전이온도의 차도 커졌고, 42에서 120 nm 의 구간에서는 전이온도 차가 입자의 크기에 따라 크게 달라지지 않았다. 120 nm 보다 더 큰 구간에서는 나노입자가 커짐에 따라 200 nm 근처에서 히스테리시스 폭이 감소하다가 곧 벌크 상에서와 같이 사라질 것으로 예상된다. 이 발견은 마그네타이트에서의 금속-절연체 전이 현상의 원리 규명에 기여할 수 있을 것이다.

주요어: 버웨이 트랜지션, 마그네타이트 나노입자, 열적 히스테리시스, 크기 효과

학번: 2014-22623